Heat Flow of the Earth

Carol A. Stein

1. INTRODUCTION

1.1 Background

Earth's evolution reflects the history of heat transfer from the interior [53, 110] via the fundamental processes of plate tectonics, conduction through continental lithosphere, and hotspot volcanism [103]. As a result, considerable attention has been directed toward understanding Earth's thermal history, the variation in the temperature field in space and time. The primary directly observable quantity for heat flow is the temperature gradient near the surface, which is in turn used to estimate the flow of heat from the interior and hence draw inferences about the thermal structure and evolution.

The challenge is the classical one of using the measured temperature and temperature gradient at an object's surface to infer the temperature field within the body, T(x,t), a function of position x and time t. Near the earth's surface, the temperature gradient is essentially vertical, so the outward heat flow q_s is

$$q_s = k\frac{dT(z)}{dz}\Big|_{z=0}, \qquad (1)$$

the product of the vertical gradient of the temperature T(z), which is most everywhere positive downwards (temperature increases with depth z), and the measured or estimated thermal conductivity of the material, k. Such heat flow measurements (or more precisely estimates based on the measured gradient) are the primary boundary conditions used to find the temperature field via the heat equation,

$$\rho C_p\left[\frac{\partial \mathbf{T}}{\partial t} + \mathbf{v}\cdot\nabla\mathbf{T}\right] = \nabla\cdot(\mathbf{k}\nabla\mathbf{T}) + \mathbf{A}, \qquad (2)$$

where ρ is the density, C_p is the specific heat, A is the heat generation, and v is the velocity of the moving material [e.g 25, 108]. This equation balances the change in the heat content of a body of material with the heat transferred by conduction, brought in by material motion, and generated within the body.

Solution of this equation, and hence deduction of temperature structure from heat flow, is a difficult and nonunique inverse problem. The variation in physical properties with depth is significant but uncertain. The expected solid state convection in the mantle has major thermal effects [e.g. 93]. As a result, although some inferences about temperature structure can be drawn based largely on heat flow, considerable additional information is drawn from seismological studies [e.g. 96], laboratory and theoretical studies of the physical properties of earth materials [e.g. 2], and modeling of convection in the earth [e.g. 48].

The measurement of heat flow has thus long been an active research area. The first reported heat flow measurements were made in oceanic lithosphere by Revelle and Maxwell [92] and in the continental lithosphere by Benfield [13] and Bullard [23]. The 1966 edition of *The Handbook of Physical Constants* [65] listed about 2000 measurements. Since then, the number of heat flow sites included in successive compilations [51, 72, 102] has increased to about 25,000 listed in the most

C. A. Stein, Department of Geological Sciences, University of Illinois at Chicago, 845 W. Taylor Street, Chicago, IL 60607-7059

Global Earth Physics
A Handbook of Physical Constants
AGU Reference Shelf 1

recent compilation [87]. Typical values of the surface temperature gradient, conductivity, radioactive heat generation, and heat flow for continents and oceans are listed in Table 1.

1.2 Measurements and Techniques

Despite its conceptual simplicity, the process of deducing heat flow from a measured gradient and conductivity values has surprising complexity. Aspects of the problem, including the historical development, are reviewed by various authors: see Louden and Wright [73] for marine studies, Beck [9] and Clauser and Huenges [30] for thermal conductivity, Beck and Balling [11] for temperatures, and Jessop [50] for both temperatures and thermal conductivity.

The vertical temperature gradient is computed from temperatures measured at known depths below the surface. However, the process of penetrating the surface to measure the temperatures disturbs the thermal structure. For marine measurements, thrusting a probe into the sediments to depths of about 5 m results in frictional heating, which takes from 5 to 30 minutes to dissipate depending mostly on the probe diameter. Prior to 1975 most heat flow values were based on single measurements, which were typically spaced about 200 km apart. Subsequently, digital instrumentation has resulted in both better temperature determinations and the capability to make closely-spaced seafloor ("pogo") penetrations more rapidly than before. Hence, local variations in the heat flux can be better identified and their cause determined. For measurements on land, temperatures are measured in drill holes using down-hole instruments lowered on a cable. For either measurements on land, or in marine boreholes (such as for the Deep-Sea Drilling Project or the Ocean Drilling Program), calculating the undisturbed temperatures is more complicated. The drilling process produces thermal perturbations due to the exchange of heat between the walls of the hole and the drilling fluid in addition to that due to the friction of drilling. With time, the temperatures slowly return to the undisturbed state. Temperature is determined either by waiting sufficient time for the site to return to the presumed equilibrium state, or measuring the change in temperature with time and then calculating an assumed equilibrium temperature [11].

Table 1. Important Parameters for Heat Flow

Property, Symbol	Approximate Range
Heat flow, q	0 - 125 mW m^{-2}
Vertical temperature gradient, dT/dz	10 to 80 °C/km
Thermal conductivity, k	
marine sediments	0.6 - 1.2 W m^{-1} K^{-1}
continental sediments	1 - 5 W m^{-1} K^{-1}
heat generation, A	0-8 10^{-6} W m^{-3}
Specific heat, C_p	0.85-1.25 kJ $kg^{-1}°C^{-1}$
Density of crustal rocks and lithosphere, ρ	2200 to 3400 kg m^{-2}

In some cases the thermal conductivity is measured either *in situ* or on a sample of the rock recovered and measured in a laboratory. In others, it is estimated based on either the known lithology or values measured from nearby sites. Initially measurements were made on recovered samples with corrections made for the differences in pressures and temperatures between the laboratory and the depth from which the sample was recovered [e.g. 91]. For marine studies the *in situ* and corrected shipboard thermal conductivity measurements agree within about 5% [49]. *In situ* determinations are preferred because the sediments have not been disturbed (especially due to water loss) by the coring and transportation. Generally, no attempt is made to measure or correct for the possibility of anisotropic values of conductivity, resulting mainly from the anisotropic structure of minerals and rocks. The anisotropy of near-surface marine sediments is negligibly small.

Typically the heat flow is calculated from the product of the average thermal conductivity and the thermal gradient. If there are significant variations of the conductivity and thermal gradient with depth (typically due to variations in lithology) the heat flow is estimated. The two most commonly used techniques are the interval method and the Bullard method [90]. The interval method can be used if there is a sufficient density of measurements with depth to assign intervals over which the values of the thermal gradient and conductivity are relatively constant. For each interval, a heat flow is calculated from the product of the average temperature gradient and an average conductivity. Then the overall mean heat flow is determined from these interval values. Alternatively, the Bullard method relies on the assumption that in the absence of significant heat sources or sinks and with one-dimensional, steady-state, conductive heat flow, the subsurface temperature T(z) is:

$$T(z) = T_0 + q_0 \sum_{i=1}^{N} (\Delta z_i / k_i), \quad (3)$$

where T_0 is the surface temperature, q_0 is the constant heat flow, and k_i is the conductivity over the ith depth

interval Δz_i. For each temperature measurement point, the thermal depth, $\sum(\Delta z_i/k_i)$, can be calculated. Then, a least-squares fit is made to the data of T(z) with the thermal depth and the slope of the line is equal to the constant heat flow.

1.3 Corrections and Climatic Effects

The goal of measuring heat flow is to determine the steady-state transfer of heat flow from below. However, the simpliest assumptions that the only uncertainties are from measurement error, the site has uniform horizontal properties and is in a thermal steady state with only conductive heat transfer, are often not the case. Local factors such as topography, sedimentation rates, and surface temperature changes, may disturb the heat flux. Given sufficient information, corrections can be made for these factors. Horizontal variations in topography and lithology cause lateral variations in the temperature and, hence surface heat flow. For the oceans, variable sediment thickness and the rough basaltic surface near the measurement site may result in a horizontal component of heat flow, largely due to the contrast between the lower conductivity of the sediments and the higher values for the basalt [e.g. 14, 54, 112]. For the marine setting the seafloor temperature usually may be assumed to be constant, but for continents the variation of the air-temperature with elevation is frequently included in modeling the steady-state vertical heat flow [e.g. 17, 44]. Another cause of non-steady state behavior is sedimentation or erosion. Rapid sedimentation conductively blankets the surface leading to lower measured heat flow [45, 63, 112]. Conversely, erosion leads to higher measured heat flow.

The magnitude and duration of surface temperature fluctuations control the magnitude and depth of the perturbation of the geotherm. Daily, annual, or climatic ($\sim 10^3$ years) time periods affect the temperatures below the land surface to order one meter, ten meters, and several hundred meters respectively. Hence, for continental regions, the depth of measurements should be greater than about 300 meters to obtain temperatures unaffected by climatic changes. The effects of surface temperature variations over time will be superimposed on the near-surface geotherm. However, higher frequency variations are suppressed relative to longer period changes. A number of techniques have been used to either correct the geotherm for a known temperature variation or to invert for long-term temperature variations [e.g. 10, 26]. For regions where historical temperature information is not available inverting for the surface temperature variations is useful. For example, geotherms from the Alaskan permafrost indicate warming trends in this century [57]. Studies for North America indicate a warming trend this century and a cooler period corresponding to the Little Ice Age that began in the 1400s and lasted into the 1800s [12, 28, 101, 115]. Given the thick water column, the bottom of the ocean is, in general, thermally stable, so variations of sea surface temperatures even as long as climatic time periods do not affect the sub-seafloor temperatures. Most of the deep ocean has sufficiently stable temperatures at the seafloor for accurate heat flow measurements without corrections [46]. However, changes in bottom water temperatures in some regions can affect the temperatures in the uppermost few meters of the sediment [e.g. 56].

2. MARINE HEAT FLOW

2.1 Background

Seafloor heat flow (Figure 1) is highest at midocean ridges, and decreases with the age of the lithosphere [62, 97, 112]. This variation is one of the key features in the models of plate tectonics, where the oceanic lithosphere cools as it spreads away from midocean ridges and reheats upon returning to the mantle at subduction zones. This cycle is a surface manifestation of terrestrial convection [e.g. 48, 83] and the primary mode of heat transfer from the earth's interior [27, 34, 99].

Average heat flow (Figure 1) is greater than about 100 mW m^{-2} for the youngest (<10 Ma) lithosphere. The mean values rapidly decrease from about 0 to 30 million years. The standard deviations are large for young lithosphere, but decrease with increasing lithospheric age. Although heat flow data is "noisy" and scattered, it is required to develop average thermal models of oceanic lithosphere. The magnitudes of depth and heat flow anomalies (the difference between observed and predicted) implicitly depend on how well the reference model reflects the average thermal state, but this is often not explicitly stated. This is especially important for models based on observed anomalies for hotspots and hydrothermal circulation.

2.2 Thermal Models

The primary constraints on models of thermal evolution are ocean depth and heat flow versus age data. The two sets of data jointly reflect the evolution with age of the geotherm in the lithosphere, because the bathymetry depends on the temperature integrated over depth and the heat flow depends on the temperature gradient at the

sea floor. The key features of the data, the decrease in heat flow and increase in seafloor depth with age, prompted two classes of models. One is the half-space model [37], where depth and heat flow vary as the square root of age and the reciprocal of the square root of age, respectively. The second is the plate model [62, 75], where the lithosphere behaves as a cooling boundary layer until it reaches ages at which the effects of the lower boundary cause the depth and heat flow curves to flatten and vary more slowly with age. The asymptotic plate thickness to which the lithosphere evolves corresponds to the depth at which the additional heat is supplied from below to prevent the continuation of half-space cooling for older ages, and above which temperature changes cause bathymetric variations.

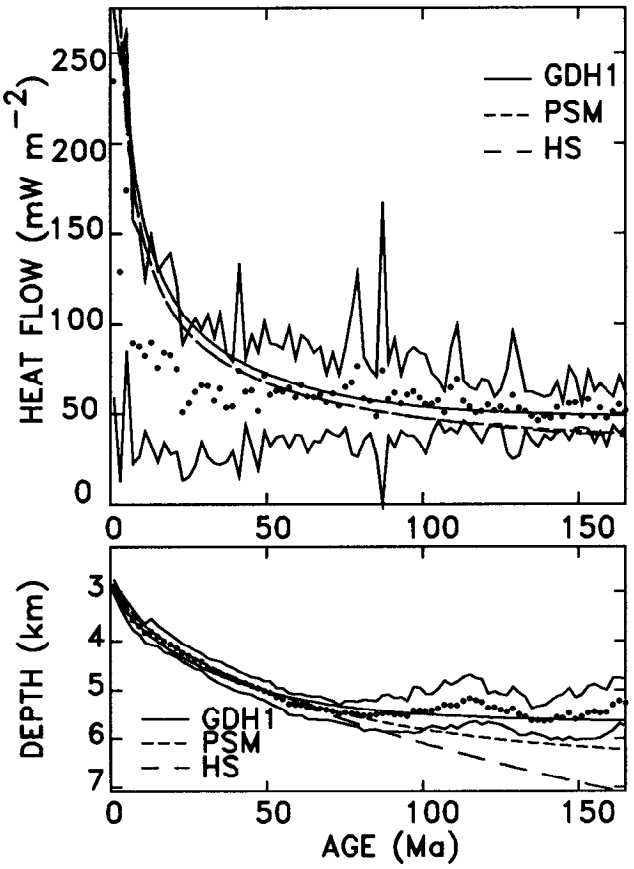

Fig. 1. Oceanic data, for the north Pacific and northwestern Atlantic Oceans, and models for heat flow and depth as a function of age. The data were averaged in two-m.y. bins, and one standard deviation about the mean value for each is shown by the envelope. The models shown are the plate model of Parsons and Sclater [84] (PSM), a cooling half-space model with the same thermal parameters (HS), and the GDH1 plate model. GDH1 (Global Depth and Heat flow), derived by joint fitting of this heat flow and bathymetry fits the data significantly better than earlier models, including the data from older lithosphere previously treated as anomalous. The improved fits imply that the oceanic lithosphere is thinner and hotter at depth than previously thought. From Stein and Stein [105].

Because of the observed flattening of depths and heat flow for older lithospheric ages, the plate model appears to be a better overall model to describe the data. Two different sets of parameters for the plate model (Table 2) have been used by Parsons and Sclater [84] (hereafter termed PSM) and Stein and Stein [105] (hereafter termed GDH1). GDH1 provides a somewhat better fit to the average depth-age and heat flow-age data using a hotter, thinner lithosphere compared to PSM (Figure 1). The heat flow predictions for GDH1 are conveniently and accurately approximated using a half-space model with the same parameters for young lithosphere, and with the first term of the series solution for older lithosphere [84]. The heat flow q (mW m^{-2}) is related to the age t (Ma) by $q(t) = 510\ t^{-1/2}$ for ages less than or equal to 55 Ma and $48 + 96 \exp(-0.0278\ t)$ for ages greater than 55 Ma. Table 3 lists the average observed heat flow for the major oceanic basins and predicted heat flow from the GDH1 model with lithospheric age.

2.3 Hydrothermal Circulation

Regardless of which thermal model is used to represent the heat flow with oceanic age, a significant discrepancy exists between the heat flow measured at the sea floor and the higher values predicted for ages 0-70 Ma (Figure 2). This is attributed to hydrothermal circulation with advective interchange between pore waters in the crust and sediments and sea water, rather than the conductive cooling assumed in the models [e.g. 68, 81]. The first detailed measurements at a ridge crest, the Galapagos Spreading Center [118], showed the convection pattern with high heat flow associated with upwelling zones located above topographic basement highs and low heat flow associated with down-flowing water above topographic basement lows, in accord with modeling [e.g. 74]. Often at sites with up-flowing water the temperature versus depth profiles are non-linear, concave upward, and at sites with down-flowing water are non-linear, concave downward [6, 19]. Subsequent studies indicate that in young lithosphere the high scatter in the values of individual heat flow measurements are presumably related to the variations in sedi-

Table 2: Plate model parameters

		GDH1	PSM
a	plate thickness	95 km	125 km
T_m	basal temperature	1450°C	1350°C
α	thermal expansion coefficient	3.1×10^{-5} °C^{-1}	3.28×10^{-5} °C^{-1}
k	thermal conductivity	3.138 W m^{-1} °C^{-1}	3.138 W m^{-1} °C^{-1}
C_p	specific heat	1.171 kJ kg^{-1} °C^{-1}	1.171 kJ kg^{-1} °C^{-1}
ρ_m	mantle density	3330 kg m^{-3}	3330 kg m^{-3}
ρ_w	water density	1000 kg m^{-3}	1000 kg m^{-3}
d_r	ridge depth	2600 m	2500 m

GDH1 model parameters from Stein and Stein [105]; PSM from Parsons and Sclater [84]

ment distribution, topographic basement relief, and local hydrological effects [1, 35, 41, 60]. Perhaps the most spectacular evidence for hydrothermal circulation is found in the "black smoker" vents of superheated water (at ~350°C) at the ridge crest with the associated biological communities [e.g. 31]. The circulation is thought to be divided into two primary stages [39, 69]. Near the ridge axis, "active" circulation occurs, during which water cools and cracks the rock, and heat is extracted rapidly by high temperature water flow [40, 85]. Once cracking ceases, "passive" circulation transports lower temperature water.

The amount of convective heat transport can be estimated from the difference between the observed and predicted heat flow [119]. Of the predicted global oceanic heat flux of 32×10^{12} W, $11 \pm 4 \times 10^{12}$ W or 34 ± 12% occurs by hydrothermal flow [107]. On a global basis ~26% of the hydrothermal heat flux occurs for ages less than 1 Ma and ~33% occurs for ages greater than 9 Ma (Table 4).

The hydrothermal water flux decreases with age and then is assumed to stop at the sealing age, defined when the observed and predicted heat flow are approximately equal. The fraction of mean observed heat flow to that expected for cooling plate models gradually rises from about .4 for the youngest lithosphere to about 1 in an approximately linear fashion until the sealing age at which it remains 1 thereafter. For the global heat flow data the sealing age is estimated at 65 ± 10 Ma (Figure 2) [107]. Because the sealing age is an average value, some water circulation may persist beyond it [e.g. 7], although the heat transfer is assumed to be primarily conductive. Within the uncertainties there are no differences for the sealing age between the major ocean basins [107].

Two mechanisms that may cause hydrothermal circulation to cease are sufficient overlying sediment to seal off the crustal convective system (and hence which no exchange of water between the crust and ocean due to the integrated permeability of the sediment column) and age-dependent properties resulting in decreasing porosity and hence permeability of the crust due to hydrothermal deposition of minerals, which also is assumed to change seismic velocity in the uppermost layer of the crust [5, 47]. It was proposed that to reach the sealing age for a given heat flow site either about 150-200 m of

Table 3. Oceanic Heat Flow Predicted from a Plate Model and Observed with Given Uncertainties due only to Data Scatter

Age (Ma)	Average Heat Flow (mW m^{-2}) Predicted (GDH1 Model)	Observed	No. Data
0-1	1020	131 ± 93	79
0-2	721	136 ± 99	195
0-4	510	128 ± 98	338
4-9	204	103 ± 80	382
9-20	136	82 ± 52	658
20-35	98	64 ± 40	535
35-52	77	60 ± 34	277
52-65	66	62 ± 26	247
65-80	60	61 ± 27	398
80-95	56	59 ± 43	443
95-110	53	57 ± 20	230
110-125	51	53 ± 13	417
125-140	50	52 ± 20	224
140-160	49	51 ± 14	242
160-180	48	52 ± 10	67

from Stein and Stein [107]

sediment covering the basement rock is required [4] or the region about the site should be well sedimented (as characterized by the sedimentary environment classification of Sclater et al. [98]). The heat flow fraction for the global data set for either sites with less than 200 m of sediment or more, or for those within the 4 categories of sedimentary environments (from poorly to well-sedimented sites) show the same linear trend of increasing heat flow fraction with age, and within the uncertainties the same sealing age [107]. Hence, probably neither ~200 m of sediment nor well sedimented sites are necessary or sufficient for crustal sealing; the effect of overlying sediment appears instead to be secondary, and is probably most important for the young lithosphere.

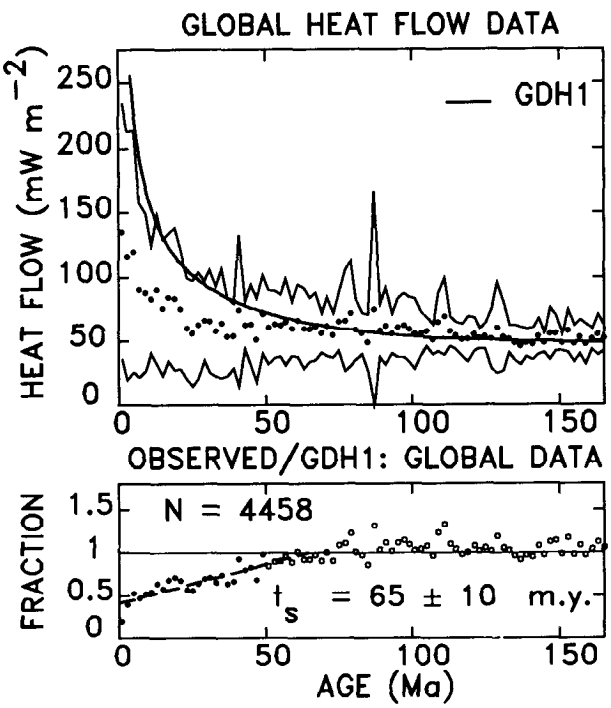

Fig. 2. Observed heat flow versus age for the global data set from the major ocean basins and predictions of the GDH1 model, shown in raw form (*top*) and fraction (*bottom*). Data are averaged in 2-m.y. bins. The discrepancy for ages < 50-70 Ma presumably indicates the fraction of the heat transported by hydrothermal flow. The fractions for ages < 50 Ma (closed circles), which were not used in deriving GDH1, are fit by a least squares line. The sealing age, where the line reaches one, is 65 ± 10 Ma [107].

The hydrothermal circulation has profound implications for the chemistry of the oceans, because sea water reacts with the crust, giving rise to hydrothermal fluid of significantly different composition [119, 120]. The primary geochemical effects are thought to result from the high temperature water flow observed at ridge axes [e.g. 31]. Nonetheless, the persistence of the heat flow discrepancy to ages of 50-70 Ma indicates that much of the hydrothermal heat flux occurs away from the ridge axis. This lower temperature off-axial flow is thought to have a much smaller geochemical effect than the near-axis flow, based on the major element chemistry of the fluid [8].

2.4 Back-Arc Spreading, Subduction Zones and Accretionary Prisms

Heat flow measurements across western Pacific subduction zones show patterns of low values from the trench axis to the volcanic arc, high and variable values over the volcanic zone and values in the back arc region similar to those for the major ocean basins of the same lithospheric age [3, 116]. However, the depths of marginal basins range from that expected to ~1 km deeper than predicted for their lithospheric ages [71, 82, 116]. Some of these depth anomalies may be due to lateral transport of heat for very small ocean basins or those formed with a short axis of spreading (<200 km) [18]. Alternatively, secondary convection associated with back-arc spreading may cause greater seafloor depths.

Accretionary prisms contain accumulations of water-saturated sediment. Initial studies with sparsely spaced measurements suggested that heat flow was lower than average [61, 116]. More recent surveys [e.g. 36, 42, 64, 122] with densely-spaced measurements indicate that heat flow is highly variable, both within a given prism and for different prisms. Many regions of high heat flow are associated with upward advection of pore fluids, typically found along faults and the bottom decollement. This process is probably a factor controlling the prism's mechanical deformation.

2.5 Hot Spots

Hawaii is the type example for hotspot studies, because of its size and isolation from other perturbing processes (including ridges and other hotspots). The observation that heat flow on the Hawaiian swell was higher than that predicted for the Parsons and Sclater [84] model was initially treated as consistent with the elevated heat flow expected for a reheating model [113] but subsequent measurements showed that its heat flow hardly differs from that for lithosphere of comparable

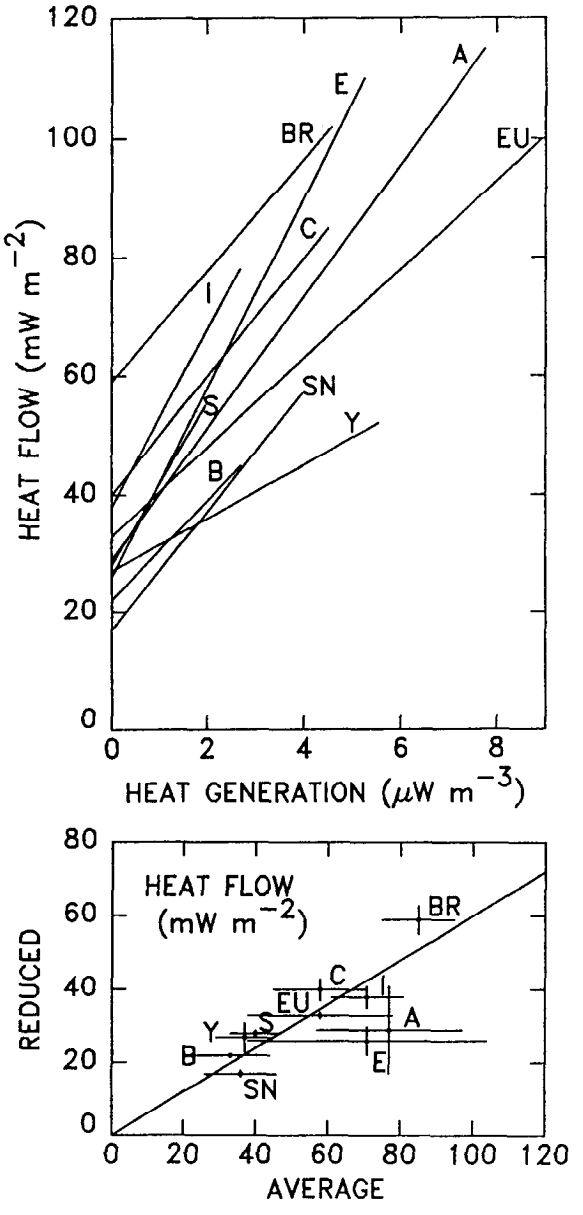

Fig. 3. (*top*) Heat flow and heat generation for various heat-flow provinces. The intercept is the reduced heat flow and the slope is "D" value. (*bottom*) Plot of reduced heat flow against average surface heat flow for the same heat-flow provinces as above. Error bars show standard deviation of the data sets. The diagonal line indicated reduced heat flow of 60% of the average heat flow, as indicated by the theory of Pollack and Chapman [82]. A=Central Australia; B=Baltic Shield; BR=Basin and Range Province; C=Atlantic Canada; E=England and Wales; EU=Eastern U.S.A.; I=India; S=Superior Province; SN=Sierra Nevada; Y=Yilgarn Block (Australia). After Jessop [50].

ages [114] and is only slightly above that expected for GDH1 [106]. A similar situation for the heat flow anomalies applies for the Bermuda [38], Cape Verde [33] and, Crozet [32] hotspots. Using the GDH1 reference model, the small heat flow anomaly thus favors a primarily dynamic origin [e.g. 70] for these swells rather than a largely thermal origin [e.g. 113]. The interpretation favoring a dynamic model is consistent with seismological data, which shows no evidence for a low velocity zone under the Hawaiian swell [121].

3. CONTINENTAL HEAT FLOW

3.1 Background

Because the oceanic lithosphere is relatively uniform in composition, and little heat is generated within it by radioactivity, oceanic heat flow is essentially a simple function of age described by the cooling plate model. In contrast, continental lithosphere is quite heterogeneous in composition, due to its much longer tectonic history. Moreover, the heat flow depends critically on radioactive heat production in the crust. The two primary effects are thus that continental heat flow is proportional to the surface crustal radioactivity in a given region, and decreases with the time since the last major tectonic event.

3.2 Radioactive (Crustal) Heat Production

The continental crust contains a relatively high density of radioactive isotopes, primarily those of uranium, thorium, and potassium [109]. Hence, within a region the heat flow depends on (1) radioactivity in the crust, (2) tectonic setting, and (3) heat flux from the mantle below. For a given area, termed a heat-flow province, the measured heat flow q varies linearly with the near-surface radioactive heat production A_o [15, 94]. Thus we define heat flow provinces characterized by q_r, the reduced heat flow, and a slope D, such that the heat flow

$$q = q_r + DA_o \tag{4}$$

(Figure 3). Initially it was suggested that the D value represents a slab of uniform heat production [94]. However, because differential erosion within the region would invalidate this explanation, the radioactive heat production is often treated as exponentially distributed with depth, z, or

$$A(z) = A_o e^{-(z/D)} \tag{5}$$

[55]. The reduced heat flow appears to be relatively uni-

Table 4. Oceanic Cumulative Heat Flux with Uncertainties due only to Data Scatter

Age (Ma)	Cumulative Heat Flux (10^{12} W) Predicted	Observed	Hydrothermal
1	3.6	0.4 ± 0.3	3.2 ± 0.3
2	5.1	1.0 ± 0.7	4.1 ± 0.7
4	7.2	1.8 ± 1.4	5.4 ± 1.4
9	11.3	3.8 ± 2.1	7.4 ± 2.1
20	15.6	6.5 ± 2.7	9.1 ± 2.7
35	19.8	9.2 ± 3.2	10.5 ± 3.2
52	22.7	11.5 ± 3.4	11.2 ± 3.4
65	24.6	13.3 ± 3.5	11.3 ± 3.5
80	26.9	15.6 ± 3.7	11.3 ± 3.7
95	28.5	17.3 ± 3.9	11.2 ± 3.9
110	29.8	18.7 ± 3.9	11.1 ± 3.9
125	30.6	19.5 ± 3.9	11.1 ± 3.9
140	31.5	20.4 ± 3.9	11.1 ± 3.9
160	31.9	20.8 ± 3.9	11.1 ± 3.9
180	32.0	21.0 ± 3.9	11.0 ± 3.9

from Stein and Stein [107]

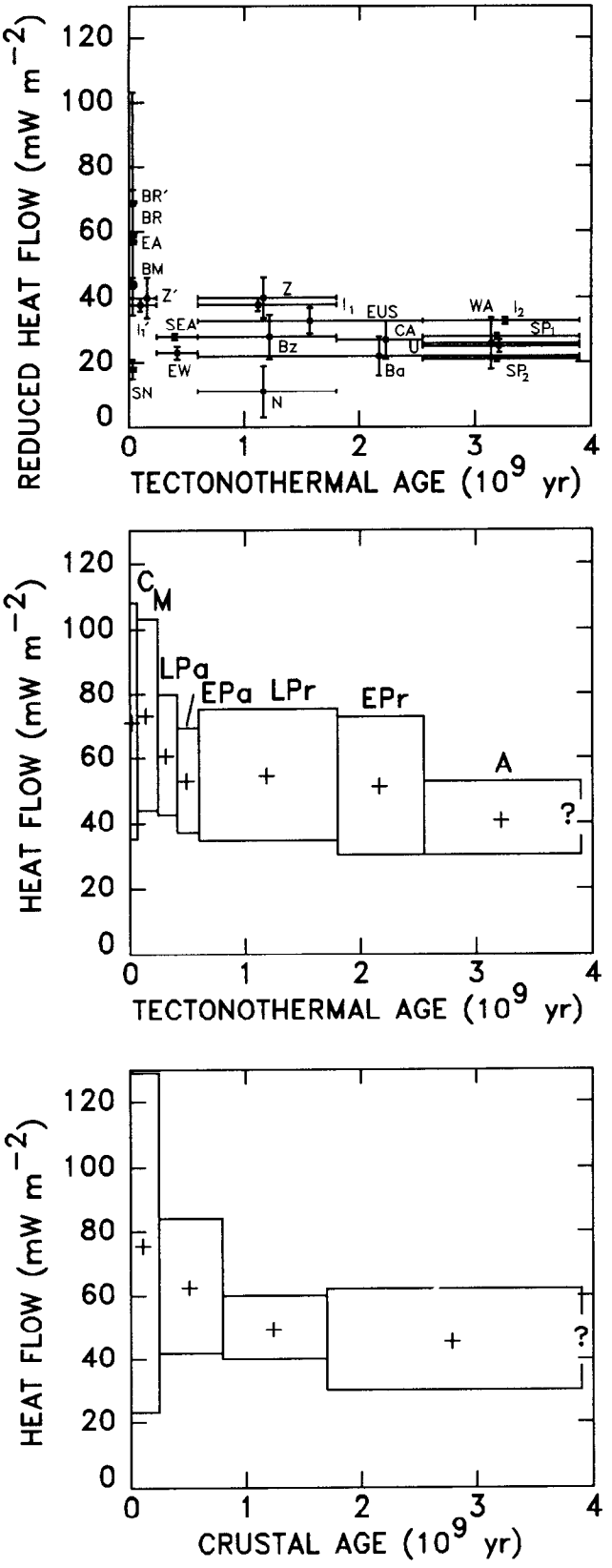

Fig. 4. For the continental heat flow data set: (*top*) Reduced heat flow as a function of age since the last tectonothermal event, for different heat flow provinces. Heat flow error bars are the uncertainties in reduced heat flow and age. BR=Basin and Range; BR'=Basin and Range; SEA=SE Appalachians; SN=Sierra Nevada; EUS=Eastern US; SP_2=Superior; SP_1=Superior, corrected; Bz=Brazilian coastal shield; Ba=Baltic shield; BM=Bohemian Massif; U=Ukraine; EW=England and Wales; N=Niger; Z=Zambia; Z'=Zambia; WA=Western Australia; CA=Central Australia; EA=Eastern Australia; I_1=Indian Shield; I'_1=Indian Shield; I_2=Archean Indian Shield. BR', EA, N, Z, and Z' were derived from assumed heat production values. (*middle*) Heat flow data averaged in groups according to age of the last tectonothermal event at each site. C=Cenozoic, M=Mesozoic, LPa=Late Paleozoic, EPa=Early Paleozoic, LPr=Late Proterozoic, EPr=Early Proterozoic, and A=Archean. (*bottom*) Heat flow data averaged in groups according to radiometric crustal age at each site. In each plot, mean heat flow values in each group are plotted as crosses at the mid-point of the age range; Boxes around the crosses indicate the age ranges for the data and standard deviations of the means. The number of data in each group are indicated by each box in parentheses. After Morgan [78].

form within the heat-flow province and can be interpreted as representing the flux from deep crustal regions or at the Moho. On average, the reduced heat flow for a province is about 0.6 of the average heat flow (Figure 3, bottom), suggesting that about 60% of the flux comes from the lower crust or below [86].

3.3 Continental Heat Flux with Age

Lee and Uyeda [66] first suggested that the continental heat flow was age dependent. Subsequent work [e.g. 89; 111] better demonstrated this relationship (Table 5). The heat flow within a given continent generally decreases with age [99]. The decrease is even clearer when the age used is the time since the last tectonothermal event (Figure 4). As with oceanic heat flow, continental measurements show a relatively large standard deviation. Local conditions such as variations in radioactive heat production, sedimentation, erosion, topography, water circulation and climate variability add to the uncertainties. One method of attempting to remove the radioactive signal is to consider the reduced heat flux versus age. This parameter rapidly decreases with tectonothermal ages from 0 and 300 Ma (Figure 4, top). For older ages (Paleozoic and Pre-Cambrian) the reduced heat flow appears to be a relatively constant, about 25 mW m^{-2} (.6 HFU) [78, 99].

3.4 Water Circulation

In contrast to the oceanic lithosphere, in which little is known about water circulation, water circulation in the continental crust has been intensively studied. Most water flow is driven by hydraulic gradients associated with variations in water table elevation and location of aquifers [e.g. 67]. Near-surface hydrothermal circulation in the continental crust can also extensively redistribute heat (for example in Iceland), thus complicating analysis of heat flow data. For example, analysis of heat flow values for the Snake River Plateau/Yellowstone hotspot are complicated by extensive ground water circulation [e.g. 20].

3.5 Extension, Hotspots and Frictional Heating

Transient heating of the continental lithosphere can occur due to tectonic processes including extension, hotspot reheating, and fault motion. Unlike oceanic hotspots where heat flow anomalies are calculated relative to that expected for the lithospheric age, continental anomalies are relative to the surrounding lithosphere not affected by the tectonic event. For example, the Snake River Plain, a topographic feature resulting from intraplate volcanism and massive magmatic intrusions in the uppermost crust starting about 16 Ma, is thought to mark the passage of the Yellowstone hotspot. Heat flow systematically increases eastward towards the recent volcanism from about 75-90 mW m^{-2} to 90-110 mW m^{-2}, well above the average North American values [16]. In Yellowstone National Park, heat flow measurements [79] and geochemical analysis [43] imply high heat loss and upper crustal temperatures in the most recently active region of volcanism.

During extension or rifting of continental lithosphere, additional heat is added to the near surface by both upward advection of heat by magmatic intrusions and volcanism, and overall thinning of the crust. The higher geotherm, subsidence, and typically rapid sedimentation, as the lithosphere cools, facilitates the production of

Table 5. Continental Heat Flow

Age (Ma)	Average heat flow (mW m^{-2})	No. Data
Subaqueous continental undifferentiated (lakes, continental shelf and slope)	77.7 ± 53.6	295
Cenozoic sedimentary and metamorphic	63.9 ± 27.5	2912
Cenozoic igneous	97.0 ± 66.9	3705
Mesozoic sedimentary and metamorphic	63.7 ± 28.2	1359
Mesozoic igneous	64.2 ± 28.8	1591
Paleozoic sedimentary and metamorphic	61.0 ± 30.2	403
Paleozoic igneous	57.7 ± 20.5	1810
Proterozoic	58.3 ± 23.6	260
Archean	51.5 ± 25.6	963

From Pollack et al. [88].

fossil fuels. Regions currently undergoing extension, such as the Basin and Range province in the western U. S. have higher average heat flow [e.g. 58, 77] and reduced heat flow compared to sites with the same average radioactive heat generation (Figures 3 and 4). High heat flow is also found where Cenozoic rifting has formed passive margins or substantially thinned continental crust prior to the onset of seafloor spreading [e.g. 22]. The effect of recent volcanism is apparent when comparing the average heat flow of Cenozoic igneous regions to Cenozoic sedimentary and metamorphic regions. Simple models of the process of lithospheric extension, which may produce a rifted continental margin or sedimentary basin [e.g. 76, 95], suggest that although heat is added to the crust, the additional heat flow will almost completely dissipate within less than 100 m.y. Hence, it is not surprising that heat flow for igneous regions are similar to that for sedimentary and metamorphic regions of Mesozoic or Paleozoic ages (Table 5).

It has been proposed that frictional heating during faulting may provide an additional source of heat to the lithosphere, proportional to the product of the velocity of the motion and the fault stress. The first such study for the San Andreas fault [21] suggested that the absence of a significant heat flow anomaly implied relatively low stresses (about 100 bars) over long periods of time. More recent heat flow measurements and modeling [58] and recent drilling results for the Cajon Pass site [59] support the initial conclusion.

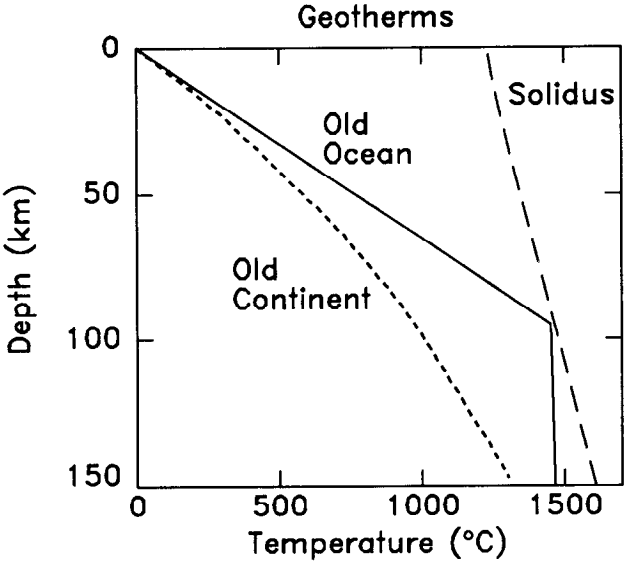

Fig. 5: Geotherms for old oceanic [105] and old continental lithosphere assuming a 50 mW m^{-2} surface heat flow [86], and a solidus [104]. Radioactive heat production in continental crust results in lower temperatures at a given depth compared with the oceanic geotherm. Continental geotherm is calculated assuming only conduction, but other modes of heat transfer may be increasingly significant at depths greater than about 70 km [86].

4. GEOTHERMS

Continental and oceanic lithosphere are composed of very different materials with different tectonic histories. The lithospheric thickness, which presumably varies as a function of age and tectonic history, can be defined based on different properties [e.g. 52], such as mechanical strength [e.g. 24], seismic velocity [e.g. 80], or thermal behavior. Possible thermal definitions include the region where conduction is the major heat transfer mechanism [e.g. 78], or the region at which temperature are less than some fraction of the expected solidus.

An interesting fact is that the average heat flow for old oceanic lithosphere and the oldest continental lithosphere is approximately the same, about 50 mW m^{-2} (Tables 3 and 5). Whether this approximate equality is a coincidence or reflects a fundamental tectonic fact is an interesting question. The issue is complicated by the challenge of estimating the geotherm given the surface heat flow. The oceanic geotherm within the lithosphere is thought to be a straightforward calculation from the cooling plate model. The geotherm changes with age until it reaches a steady state, at which time the geotherm is essentially linear with depth, with a slope equal to the surface heat flow divided by the thermal conductivity (Figure 5), because the radioactive heat production is small. Beneath the plate a shallow adiabatic gradient, ~0.3°C/km, is generally assumed [108]. The continental geotherm, however, depends on the assumed the variation of radioactive heat production with depth. Assuming only conductive heat transfer, steady-state conditions and given two boundary conditions, the surface heat flow q_s and a surface temperature T_s, the geotherm T(z) is

$$T(z) = T_s + \frac{q_s}{k}z - \frac{\rho A}{2k}z^2. \quad (6)$$

Hence for a given surface heat flow and temperature, the temperatures at depth will be lower the higher the radioactive heat production. The continental geotherm in Figure 5 [86] assumes a heat production of 2.5

10^{-6}Wm^{-3} for the upper 8 km, an order of magnitude less for the lower crust and even less for the mantle below. The resulting geotherm suggests that the thermal thickness of old continental lithosphere exceeds that of old oceanic lithosphere. These relative thicknesses agree with some assessments [e.g. 52] but is opposite the conclusions of Sclater et al. [99, 100] who suggested approximate equality of the geotherms, in part due to their cooler oceanic model. Given the uncertainties in the estimated geotherms, due in large part to the largely unknown variation in both heat production and other physical properties with depth, the question of what the equality of old continental and oceanic heat flow means remains unresolved and possibly even unresolvable.

5. GLOBAL HEAT LOSS

Prior to the development of plate tectonics, it was thought that the average oceanic heat flow might be lower than that for the continents because the basalt of the oceanic crust has less radioactive isotopes compared to continental material. In fact, the average oceanic heat flow (101 mW m^{-2}) is higher than for continents (65 mW m^{-2}) because of the plate cooling process. Thus oceanic and continental heat flow account for about 70% and 30% respectively of the integrated surface heat flux (Table 6), yielding a global average of 87 mW m^{-2}

Table 6. Global Heat Flow

Region	Mean heat flow (mW m^{-2})	No. Data
Oceanic	101 ± 2.2	9864
Continental	65 ± 1.6	10337
Global	87 ± 2.0	20201

Total global heat loss= 4.42 ± 0.10 × 10^{13} W
From Pollack et al. [88].

or a total heat loss of 4.42 × 10^{13} W [88]. These values are about 4-8% higher than previous analyses of the global heat flow data set [e.g. 34, 99, 117]. The more difficult to estimate total heat production within the earth, 27.5 × 10^{12} W (from 3.47 × 10^{-8} cal g^{-1} yr^{-1} [Table 10; 109]), is often divided by the global heat loss, giving a value of about 0.6. This quantity, known as the Urey ratio, indicates that radioactivity can account for about 60% of the earth's heat output, and hence is important for modeling the thermal evolution of the earth [29].

Acknowledgments: I thank Henry Pollack for providing a preprint of his paper and Seth Stein and an anonymous reviewer for useful comments. This research was supported by NSF grant EAR-9219302.

REFERENCES

1. Abbott, D. H., C. A. Stein, and O. Diachok, Topographic relief and sediment thickness: their effects on the thermal evolution of oceanic lithosphere, *Geophys. Res. Lett., 19,* 1975-1978, 1992.
2. Akaogi, M., E. Ito, and A. Navrotsky, Experimental and thermodynamic constraints on phase transitions of mantle minerals (abstract), *Abstr. 28th Internat. Geol. Cong., 1,* 26, 1989.
3. Anderson, R. N., 1980 Update of heat flow in the East and Southeast Asian seas, in *The Tectonic and Geologic Evolution of Southeast Asian Seas and Islands, Geophysical Monograph Series, 23,* edited by D. E. Hayes, pp. 319–326, Am. Geophys. Un., Washington, D. C., 1980.
4. Anderson, R. N., and M. A. Hobart, The relation between heat flow, sediment thickness, and age in the eastern Pacific, *J. Geophys. Res., 81,* 2968–2989, 1976.
5. Anderson, R. N., M. G. Langseth, and J. G. Sclater, The mechanisms of heat transfer through the floor on the Indian Ocean, *J. Geophys. Res., 82,* 3391–3409, 1977.
6. Anderson, R. N., M. G. Langseth, and M. A. Hobart, Geothermal convection through oceanic crust and sediments in the Indian Ocean, *Science, 204,* 828–832, 1979.
7. Anderson, R. N., and J. N. Skilbeck, Oceanic heat flow, in *The Oceanic Lithosphere, The Seas 7,* edited by C. Emiliani, pp. 489–523, Wiley-Interscience, New York, 1981.
8. Baker, P. A., P. M. Stout, M. Kastner, and H. Elderfield, Large-scale lateral advection of seawater through oceanic crust in the central equatorial Pacific, *Earth Planet. Sci. Lett., 105,* 522–533, 1991.
9. Beck, A. E., Methods for determining thermal conductivity and thermal diffusivity, in *Handbook of terrestrial heat-flow density determination,* edited by R. Haenel, L. Rybach and L. Stegena, pp. 87–124, Kluwer Academic Publishers, Dordrecht, 1988.
10. Beck, A. E., Inferring past climate change from subsurface temperature profiles: some problems and methods, *Palaeography, Palaeoclimatology, Palaeoecology (Global and Planetary Change Section), 98,* 73–80, 1992.
11. Beck, A. E., and N. Balling, Deter-

mination of virgin rock temperatures, in *Handbook of terrestrial heat-flow density determination,* edited by R. Haenel, L. Rybach and L. Stegena, pp. 59–85, Kluwer Academic Publishers, Dordrecht, 1988.

12. Beltrami, H., and J-C Mareshal, Ground temperature histories for central and eastern Canada from geothermal measurements: Little Ice Age signature, *Geophys. Res. Lett., 19,* 689–692, 1992.
13. Benfield, A. E., Terrestrial heat flow in Great Britian, *Proc. Roy. Soc. London, A, 173,* 428–450, 1939.
14. Birch, F., Low values of oceanic heat flow, *J. Geophys. Res., 72,* 2261–2262, 1967.
15. Birch, F., R. F. Roy, and E. R. Decker, Heat flow and the thermal history in New England and New York, in *Studies of Appalachian geology, northern and maritime,* edited by E. Zen, W. S. White, J. B. Hadley and J. B. Thompson, pp. 437–451, Interscience, 1968.
16. Blackwell, D. D., Regional implications of heat flow of the Snake River Plain, Northwestern United States, *Tectonophysics, 164,* 323–343, 1989.
17. Blackwell, D. D., J. L. Steele, and C. A. Brott, The terrain effect on terrestrial heat flow, *J. Geophys. Res., 85,* 4757–4772, 1980.
18. Boerner, S. T., and J. G. Sclater, Approximate solutions for heat loss in small marginal basins, in *CRC Handbook of Seafloor Heat Flow,* edited by J. A. Wright and K. E. Louden, pp. 231–255, CRC Press, Inc., Boca Raton, 1989.
19. Bredehoeft, J.D., and I.S. Papadopulos, Rates of vertical groundwater movement estimated from the earth's thermal profile, *Water Resour. Res., 2,* 325–328, 1965.
20. Brott, C. A., D. D. Blackwell, and J. P. Ziagos, Thermal and tectonic implications of heat flow in the Eastern Snake River Plain, Idaho, *J. Geophys. Res., 86,* 11,709–11,734, 1981.
21. Brune, J. N., T. L. Henyey, and R. F. Roy, Heat flow, stress, and rate of slip along the San Andreas Fault, California, *J. Geophys. Res., 74,* 3821–3827, 1969.
22. Buck, W. R., F. Martinez, M. S. Steckler, and J. R. Cochran, Thermal consequences of lithospheric extension: pure and simple, *Tectonics, 7,* 213–234, 1988.
23. Bullard, E. C., Heat flow in South Africa, *Proc. Roy. Soc. London, A, 173,* 474–502, 1939.
24. Calmant, S., J. Francheteau, and A. Cazenave, Elastic layer thickening with age of the oceanic lithosphere a tool for prediction of age of volcanoes or oceanic crust, *Geophys. J. Int., 100,* 59–67, 1990.
25. Carslaw, H. S., and J. C. Jaeger, *Conduction of heat in solids,* Oxford University Press, Oxford, 510 pp., 1959.
26. Cermak, V., Underground temperature and inferred climatic temperature of the past millennium, *Palaeogeogr., Palaeoclimatol., Palaeoceol., 10,* 1–19, 1971.
27. Chapman, D. S., and H. N. Pollack, Global heat flow: a new look, *Earth Planet. Sci. Lett., 28,* 23–32, 1975.
28. Chapman, D. S., T. J. Chisholm, and R. N. Harris, Combining borehole temperature and meteorological data to constrain past climate change, *Palaeography, Palaeoclimatology, Palaeoecology (Global and Planetary Change Section), 98,* 269–281, 1992.
29. Christensen, U., The energy budget of the earth, in *The encyclopedia of solid earth geophysics, Encyclopedia of Earth Sciences,* edited by D. E. James, pp. 372–378, Van Nostrand Reinhold Company, New York, 1989.
30. Clauser, C., and E. Huenges, Thermal conductivity of rocks and minerals, *AGU Handbook of Physical Constants,*, Ed., edited by T. J. Ahrens, Am. Geophys. Un., Washington, D.C., this volume, 1994.
31. Corliss, J. B., J. Dymond, L. I. Gordon, J. M. Edmond, R. P. Von Herzen, R. D. Ballard, K. L. Green, D. Williams, A. L. Brainbridge, K. Crane, and T. H. van Andel, Submarine thermal springs on the Galapagos rift, *Science, 203,* 1073–1083, 1979.
32. Courtney, R. C., and M. Recq, Anomalous heat flow near the Crozet Plateau and mantle convection, *Earth Planet. Sci. Lett., 79,* 373–384, 1986.
33. Courtney, R. C., and R. S. White, Anomalous heat flow and geoid across the Cape Verde Rise: evidence for dynamic support from a thermal plume in the mantle, *Geophys. J. R. astron. Soc., 87,* 815–867, 1986.
34. Davies, G. F., Review of oceanic and global heat flow estimates, *Rev. Geophys. Space Phys., 18,* 718–722, 1980.
35. Davis, E. E., D. S. Chapman, C. B. Forster, and H. Villinger, Heat-flow variations correlated with buried basement topography on the Juan de Fuca Ridge, *Nature, 342,* 533–537, 1989.
36. Davis, E. E., R. D. Hyndman, and H. Villinger, Rates of fluid expulsion across the northern Cascadia accretionary prism: Constraints from new heat flow and multichannel seismic reflection data, *J. Geophys. Res., 95,* 8869–8890, 1990.
37. Davis, E. E., and C. R. B. Lister, Fundamentals of ridge crest topography, *Earth Planet. Sci. Lett., 21,* 405–413, 1974.
38. Detrick, R. S., R. P. Von Herzen, B. Parsons, D. Sandwell, and M. Dougherty, Heat flow observations on the Bermuda Rise and thermal models of midplate swells, *J. Geophys. Res., 91,* 3701–3723, 1986.
39. Fehn, U., and L. M. Cathles, The influence of plate movement on the evolution of hydrothermal convection cells in the oceanic crust, *Tectonophysics, 125,* 289–312, 1986.
40. Fehn, U., K. E. Green, R. P. Von Herzen, and L. M. Cathles, Numerical models for the hydrothermal field at the Galapagos spreading center, *J. Geophys. Res., 88,* 1033–1048, 1983.
41. Fisher, A. T., Becker, K., and T. N. Narasimhan, Off-axis hydrothermal circulation: parametric tests of a refined model of processes at Deep

Sea Drilling Project/Ocean Drilling Program site 504, J. Geophys. Res., 99, 3097-3121, 1994.

42. Foucher, J. P., X. Le Pichon, S. Lallemant, M. A. Hobart, P. Henry, M. Benedetti, G. K. Westbrook, and M. G. Langseth, Heat flow, tectonics, and fluid circulation at the toe of the Barbados Ridge accretionary prism, *J. Geophys. Res., 95,* 8859–8867, 1990.
43. Fournier, R. O, Geochemistry and dynamics of the Yellowstone National Park hydrothermal system, in *Ann. Rev. Earth Planet. Sci., 17,* edited by G. W. Wetherill, A. L. Albee and F. G. Stehli, pp. 13–53, 1989.
44. Henry, S. G., and H. N. Pollack, Heat flow in the presence of topography: numerical analysis of data ensembles, *Geophysics, 50,* 1335–1341, 1985.
45. Hutchison, I., The effects of sedimentation and compaction on oceanic heat flow, *Geophys. J. R. astr. Soc., 82,* 439–459, 1985.
46. Hyndman, R. D., M. G. Langseth, and R. P. Von Herzen, Deep Sea Drilling project geothermal measurements: a review, *Rev. Geophys., 25,* 1563-1582, 1987.
47. Jacobson, R. S., Impact of crustal evolution on changes of the seismic properties of the uppermost ocean crust, *Rev. Geophysics, 30,* 23–42, 1992.
48. Jarvis, G. T., and W. R. Peltier, Convection models and geophysical observations, in *Mantle Convection,* edited by W. R. Peltier, pp. 479–594, Gordon and Breach, New York, 1989.
49. Jemsek, J., and R.P. Von Herzen, Measurement of *in situ* sediment thermal conductivity: continuous-heating method with outrigged probes, in *Handbook of seafloor heat flow,* edited by J.A. Wright and K.E. Louden, pp. 91–120, CRC Press, Inc., Boca Raton, Florida, 1989.
50. Jessop, A. M., *Thermal geophysics, Developments in solid earth geophysics* 17, 306 pp., Elsevier Science Publishers B. V., Amsterdam, 1990.
51. Jessop, A. M., M. A. Hobart, and J. G. Sclater, *The world heat flow data collection-- 1975, Geothermal Series 5,* Energy, Mines and Resources, Earth Physics Branch, Ottawa, Canada, 1976.
52. Jordan, T. H., Global tectonic regionalization for seismological data analysis, *Bull. Seismol. Soc. Am., 71,* 1131–1141, 1981.
53. Kaula, W. M., Absolute plate motions by boundary velocity minizations, *J. Geophys. Res., 80,* 244–248, 1975.
54. Lachenbruch, A.H., Rapid estimation of the topographic disturbances to superficial thermal gradients, *Rev. Geophys. Space Phys., 6,* 365–400, 1968.
55. Lachenbruch, A. H., Crustal temperature and heat production: Implications of the linear heat-flow relation, *J. Geophys. Res., 75,* 3291–3300, 1970.
56. Lachenbruch, A. H., and B. V. Marshall, Heat flow and water temperature fluctuations in the Denmark Strait, *J. Geophys. Res., 73,* 5829–5842, 1968.
57. Lachenbruch, A. H., and B. V. Marshall, Changing climate: geothermal evidence from permafrost in the Alaskan Arctic, *Science, 234,* 689–696, 1986.
58. Lachenbruch, A. H., and J. H. Sass, Heat flow and energetics of the San Andreas Fault zone, *J. Geophys. Res., 85,* 6185–6223, 1980.
59. Lachenbruch, A. H., and J. H. Sass, Heat flow from Cajon Pass, fault strength, and tectonic implications, *J. Geophys. Res., 97,* 4995–5015, 1992.
60. Langseth, M., K. Becker, R. P. Von Herzen, and P. Schultheiss, Heat and fluid flux through sediment on the flank of the mid-Atlantic ridge, *Geophys. Res. Lett., 19,* 517–520, 1992.
61. Langseth, M. G., and R. P. Von Herzen, Heat flow through the floor of the world oceans, in *The Sea, 4,* edited by A. E. Maxwell, pp. 299–352, Interscience, New York, 1970.
62. Langseth, M. G., X. Le Pichon, and M. Ewing, Crustal structure of the mid-ocean ridges, 5, Heat flow through the Atlantic Ocean floor and convection currents, *J. Geophys. Res., 71,* 5321–5355, 1966.
63. Langseth, M. G., M. A. Hobart, and K. Horai, Heat flow in the Bering Sea, *J. Geophys. Res., 85,* 3740–3750, 1980.
64. Le Pichon, X., P. Henry, and S. Lallemant, Accretion and erosion in subduction zones: The role of fluids, in *Annu. Rev. Earth Planet. Sci., 21,* edited by G. W. Wetherill, A. L. Albee and K. C. Burke, pp. 307–331, 1993.
65. Lee, W. H. K., and S. P. Clark, Jr., Heat flow and volcanic temperatures, in *Handbook of Physical Constants, Geol. Soc. Am. Mem. 97,* edited by S. P. Clark, Jr., pp. 483–511, 1966.
66. Lee, W. H. K., and S. Uyeda, Review of heat flow data, in *Terrestrial heat flow, Geophys. Monograph 8* edited by W. H. K. Lee, pp. 87–190, American Geophysical Union, Washington, D.C., 1965.
67. Lewis, T. J., and A. E. Beck, Analysis of heat-flow data- detailed observations in many holes in a small area, *Tectonophys., 41,* 41–59, 1977.
68. Lister, C. R. B., On the thermal balance of a mid-ocean ridge, *Geophys. J. R. astron. Soc., 26,* 515–535, 1972.
69. Lister, C. R. B., "Active" and "passive" hydrothermal systems in the oceanic crust: predicted physical conditions, in *The dynamic environment of the ocean floor,* edited by K. A. Fanning and F. T. Manheim, pp. 441–470, University of Miami, 1982.
70. Liu, M., and C. G. Chase, Evolution of midplate hotspot swells: numerical solutions, *J. Geophys. Res., 94,* 5571–5584, 1989.
71. Louden, K. E., The crustal and lithospheric thickness of the Philippine Sea as compared to the Pacific, *Earth Planet. Sci. Lett., 50,* 275–288, 1980.
72. Louden, K. E., Marine heat flow

data listing, Appendix B, in *Handbook of seafloor heat flow,* edited by J. A. Wright and K. E. Louden, pp. 325–485, CRC Press, Inc., Boca Raton, Florida, 1989.

73. Louden, K. E., and J. A. Wright, Marine heat flow data: A new compilation of observations and brief review of its analysis, in *CRC Handbook of Seafloor Heat Flow,* edited by J. A. Wright and K. E. Louden, pp. 3–67, CRC Press, Inc., Boca Raton, 1989.
74. Lowell, R. P., Topographically driven subcritical hydrothermal convection in the oceanic crust, *Earth Planet. Sci. Lett., 49,* 21–28, 1980.
75. McKenzie, D. P., Some remarks on heat flow and gravity anomalies, *J. Geophys. Res., 72,* 6261–6273, 1967.
76. McKenzie, D. P., Some remarks on the development of sedimentary basins, *Earth Planet. Sci. Lett., 40,* 25–32, 1978.
77. Morgan, P., Constraints on rift thermal processes from heat flow and uplift, *Tectonophysics, 94,* 277–298, 1983.
78. Morgan, P., The thermal structure and thermal evolution of the continental lithosphere, in *Structure and evolution of the continental lithosphere, Physics and chemistry of the earth 15,* edited by H. N. Pollack and V. R. Murthy, pp. 107–193, Pergamon Press, Oxford, 1984.
79. Morgan, P., D. D. Blackwell, R. E. Spafford, and R. B. Smith, Heat flow measurements in Yellowstone Lake and the thermal structure of the Yellowstone Caldera, *J. Geophys. Res., 82,* 3719–3732, 1977.
80. Nishimura, C., and D. Forsyth, The anisotropic structure of the upper mantle in the Pacific, *Geophys. J. R. Astr. Soc., 96,* 203–226, 1989.
81. Palmason, G., On heat flow in Iceland in relation to the Mid-Atlantic Ridge, *Iceland and mid-ocean ridges- Report of a symposium,* pp. 111–127, Geoscience Society of Iceland, Reykjavik, 1967, Reykjavik, Iceland, 1967.
82. Park, C.-H., K. Tamaki, and K. Kobayashi, Age-depth correlation of the Philippine Sea back-arc basins and other marginal basins in the world, *Tectonophys., 181,* 351–371, 1990.
83. Parsons, B., and F. M. Richter, Mantle convection and the oceanic lithosphere, in *Oceanic Lithosphere, (The Sea, vol. 7),* edited by C. Emiliani, pp. 73–117, Wiley-Interscience, New York, 1981.
84. Parsons, B., and J. G. Sclater, An analysis of the variation of ocean floor bathymetry and heat flow with age, *J. Geophys. Res., 82,* 803–827, 1977.
85. Patterson, P. L., and R. P. Lowell, Numerical models of hydrothermal circulation for the intrusion zone at an ocean ridge axis, in *The Dynamic Environment of the Ocean Floor,* edited by K. A. Fanning and F. T. Manheim, pp. 471–492, University of Miami, 1982.
86. Pollack, H. N., and D. S. Chapman, On the regional variation of heat flow, geotherms, and the thickness of the lithosphere, *Tectonophysics, 38,* 279–296, 1977.
87. Pollack, H. N., S. J. Hurter, and J. R. Johnston, Global heat flow data set, World Data Center A for Solid Earth Geophysics, NOAA E/GCI, 325 Broadway, Boulder, CO 80303, USA, 1992.
88. Pollack, H. N., S. J. Hurter, and J. R. Johnston, Heat loss from the earth's interior: analysis of the global data set, *Rev. Geophys., 31,* 267–280, 1993.
89. Polyak, B. G., and Y. A. Smirnov, Relationship between terrestrial heat flow and the tectonics of continents, *Geotectonics, 4,* 205–213, 1968.
90. Powell, W. G., D. S. Chapman, N. Balling, and A. E. Beck, Continental heat-flow density, in *Handbook of Terrestrial Heat-Flow Determination,* edited by R. Haenel, L. Rybach and L. Stegena, pp. 167–222, Kluwer Academic Publishers, Hordrecht, 1988.
91. Ratcliffe, E. H., The thermal conductivities of ocean sediments, *J. Geophys. Res., 65,* 1535–1541, 1960.
92. Revelle, R., and A. E. Maxwell, Heat flow through the floor of the eastern north Pacific Ocean, *Nature, 170,* 199–200, 1952.
93. Richter, F. M., Kelvin and the age of the earth, *J. Geol., 94,* 395–401, 1986.
94. Roy, R. F., D. D. Blackwell, and F. Birch, Heat generation of plutonic rocks and continental heat flow provinces, *Earth Planet. Sci. Lett., 5,* 1–12, 1968.
95. Royden, L., and C. E. Keen, Rifting process and thermal evolution of the continental margin of eastern Canada determined from subsidence curves, *Earth Planet. Sci. Lett., 51,* 343–361, 1980.
96. Sato, H., I. S. Sacks, and T. Murase, Use of laboratory velocity data for estimating temperature and partial melt fraction in the low velocity zone: comparison with heat flow and electrical conductivity studies, *J. Geophys. Res., 94,* 5689–5704, 1989.
97. Sclater, J. G., and J. Francheteau, The implications of terrestrial heat flow observations on current tectonic and geochemical models of the crust and upper mantle of the Earth, *Geophys. J. R. astron. Soc., 20,* 509–542, 1970.
98. Sclater, J. G., J. Crowe, and R. N. Anderson, On the reliability of oceanic heat flow averages, *J. Geophys. Res., 81,* 2997–3006, 1976.
99. Sclater, J. G., C. Jaupart, and D. Galson, The heat flow through oceanic and continental crust and the heat loss of the Earth, *Rev. Geophys. Space Phys., 18,* 269–311, 1980.
100. Sclater, J. G., B. Parsons, and C. Jaupart, Oceans and continents: Similarities and differences in the mechanisms of heat loss, *J. Geophys. Res., 86,* 11,535–11,552, 1981.
101. Shen, P. Y., and A. E. Beck, Paleoclimate change and heat flow density inferred from temperature data in the Superior Province of the Canadian Shield, *Palaeography, Palaeoclimatology, Palaeoecology (Global and Planetary Change Section), 98,* 143–165, 1992.

102. Simmons, G., and K. Horai, Heat flow data, 2, *J. Geophys. Res., 73,* 6608–6629, 1968.
103. Solomon, S. C., and J. W. Head, Mechanisms for lithospheric heat transport on Venus: Implications for tectonic style and volcanism, *J. Geophys. Res., 87,* 9236–9246, 1982.
104. Stacey, F. D., *Physics of the Earth (3rd Edition),* Brookfield Press, Kenmore, 1992.
105. Stein, C. A., and S. Stein, A model for the global variation in oceanic depth and heat flow with lithospheric age, *Nature, 359,* 123–129, 1992.
106. Stein, C. A., and S. Stein, Constraints on Pacific midplate swells from global depth-age and heat flow-age models, in *The Mesozoic Pacific, Geophys. Monogr. Ser. vol. 77,* edited by M. Pringle, W. W. Sager, W. Sliter and S. Stein, pp. 53–76, AGU, Washington, D. C., 1993.
107. Stein, C. A., and S. Stein, Constraints on hydrothermal heat flux through the oceanic lithosphere from global heat flow, *J. Geophys. Res., 99,* 3081-3095, 1994.
108. Turcotte, D. L., and G. Schubert, *Geodynamics: applications of continuum physics to geological problems,* John Wiley, New York, 1982.
109. Van Schmus, W. R., Natural radioactivity of the crust and mantle, *AGU Handbook of Physical Constants,* , Ed., edited by T. J. Ahrens, Am. Geophys. Un., Washington, D.C., this volume, 1994.
110. Verhoogen, J., *Energetics of the Earth,* National Academy of Sciences, Washington, D.C., 1980.
111. Vitorello, I., and H. N. Pollack, On the variation of continental heat flow with age and the thermal evolution of continents, *J. Geophys. Res., 85,* 983–995, 1980.
112. Von Herzen, R. P., and S. Uyeda, Heat flow through the eastern Pacific ocean floor, *J. Geophys. Res., 68,* 4219–4250, 1963.
113. Von Herzen, R. P., R. S. Detrick, S. T. Crough, D. Epp, and U. Fehn, Thermal origin of the Hawaiian swell: Heat flow evidence and thermal models, *J. Geophys. Res., 87,* 6711–6723, 1982.
114. Von Herzen, R. P., M. J. Cordery, R. S. Detrick, and C. Fang, Heat flow and the thermal origin of hotspot swells: the Hawaiian swell revisited, *J. Geophys. Res., 94,* 13,783–13,799, 1989.
115. Wang, K., T. J. Lewis, and A. M. Jessop, Climatic changes in central and eastern Canada inferred from deep borehole temperature data, *Palaeogeolgraphy, Palaeoclimatology, Palaeocology (Global and Planetary Change Section), 98,* 129–141, 1992.
116. Watanabe, T., M. G. Langseth, and R. N. Anderson, Heat flow in back-arc basins of the western Pacific, in *Island Arcs, Deep Sea Trenches, and Back-Arc Basins,* edited by M. Talwani and W. Pitman, III, pp. 137–162, American Geophysical Union, Washington, D.C., 1977.
117. Williams, D. L., and R. P. Von Herzen, Heat loss from the earth: New estimate, *Geology, 2,* 327–328, 1974.
118. Williams, D. L., R. P. Von Herzen, J. G. Sclater, and R. N. Anderson, The Galapagos spreading centre: Lithospheric cooling and hydrothermal circulation, *Geophys. J. R. astr. Soc., 38,* 587–608, 1974.
119. Wolery, T. J., and N. H. Sleep, Hydrothermal circulation and geochemical flux at mid-ocean ridges, *J. Geol., 84,* 249–275, 1976.
120. Wolery, T. J., and N. H. Sleep, Interactions of geochemical cycles with the mantle, in *Chemical Cycles in the Evolution of the Earth,* edited by C. B. Gregor, R. M. Garrels, F. T. Mackenzie and J. B. Maynard, pp. 77–103, John Wiley and Sons, Inc., New York, 1988.
121. Woods, M. T., J.-J. Leveque, E. A. Okal, and M. Cara, Two-station measurements of Rayleigh wave group velocity along the Hawai'ian swell, *Geophys. Res. Lett., 18,* 105–108, 1991.
122. Yamano, M., J. P. Foucher, M. Kinoshita, A. Fisher, and R. D. Hyndman, Heat flow and fluid flow regime in the western Nankai accretionary prism, *Earth Planet. Sci. Lett., 109,* 451–462, 1992.